Soft Matter

Accepted Manuscript

ROYAL SOCIETY OF CHEMISTRY

www.rsc.org/softmatter

Linear model of a T-junction microdroplet generator for precise control of droplet size

Wen Zeng, Songjing Li* and Zuwen Wang
Department of Fluid Control and Automation, Harbin Institute of Technology, Harbin, China

For a T-junction microdroplet generator, a mathematical model which can describe the linear relation between the droplet length and the flow-rate ratio for different geometries of the T-junctions is demonstrated. For different viscosity of the fluids, the droplet length as a function of the flow-rate ratio is measured experimentally. We observe that the droplet length is a linear function of the flow-rate ratio for different Capillary number ($C_a \le 0.1$), while the droplet length varies nonlinearly with the flow-rate ratio at a high Capillary number ($0.1 \le C_a \le 1.0$). Particularly, two geometries of the T-junction microchannels are designed for droplet formation, and good agreements are found between the predicted and the measured droplet length for low Capillary numbers. More importantly, the linear model of droplet formation is only determined by the geometry of a T-junction and independent of the viscosity of the fluids for $C_a \le 0.1$. As a result, our linear model can be experimentally validated, and the size of the droplets can be precisely predicted in a T-junction.

1. Introduction

Droplet microfluidics has been widely applied for medical, biological and chemical research [1-5]. In particular, individual droplets with volume ranging from 10 pL to 100 nL are formed in the microchannels, and the control precision of the droplet size is quite meaningful for the applications of droplet microfluidic systems [6-10]. According to the literature, both flow-rate- and pressure-driven pumping methods have been applied for droplet formation, and the size of the droplets as a function of the flow-rate ratio or pressure ratio is measured experimentally [11]. In a T-junction microdroplet generator, it was observed that the droplet size is approximately a linear function of the flow-rate ratio for low Capillary numbers ($C_a \le 0.1$) [12-14]. Particularly, for a typical microchannel, a 10% increase in the pressure ratio can induce nearly 4 fold increase in droplet size, while a 10% increase in the flow-rate ratio only leads to less than 30% increase in droplet size [15]. Therefore, the droplet size is less sensitive to the variation of the flow-rate ratio compared with that of the pressure ratio, and the control accuracy of the flow rates of the fluids directly affects the stability and precision of droplet formation [16]. Besides the T-junctions, the principle of droplet formation has also been studied theoretically and experimentally in a flow-focusing microchannel [17-19]. Both for high ($0.1 \le C_a \le 1.0$) and low

($C_a \le 0.1$) Capillary numbers, it was observed that the size of the droplets varies nonlinearly with the flow-rate ratio [20,21]. Especially for $0.1 \le C_a \le 1.0$, the drop size also varies with the viscosity of the fluids for a specific flow-rate ratio [22]. Due to the inherent nonlinearity between the droplet size and the flow-rate ratio in a microfluidic flow-focusing, the size of droplets can be controlled and predicted more easily in the T-junctions.

To date, for the T-junctions, the linear relation between the droplet size and the flow-rate ratio was obtained mainly from experimental measurements, and the coefficients of the linear relation were estimated by linear fitting of the experimental data [23,24]. Though some researchers [13,25] has established the model of the droplet volume during droplet generation and verified their mathematical model experimentally, the experiments of droplet formation were performed only for a narrow range of Capillary numbers ($C_a \le 0.01$). Moreover, to obtain the droplet volume during droplet formation, we need to take the image of the droplets by a high speed camera and choose the method of online image processing [26], which is much more complicated and time-consuming compared with the measurements of the droplet length by electrical detection [27]. Meanwhile, to our knowledge, the study of the effects of the geometrical parameters of the T-junction microchannel on the principle of droplet formation has been mostly qualitative.

In this paper, a mathematical model which can describe the linear relation between the droplet length and the flow-rate ratio for different geometries of the T-junctions is studied theoretically and experimentally. For a typical T-junction, the coefficients of the linear model can be calculated by its geometrical parameters. By varying the viscosity of the silicone oil, the droplet length as a linear function of the flow-rate ratio is measured experimentally. In particular, two geometries of the T-junction microchannels are designed for our experiments and the measured droplet length are compared with the predicted value as the flow-rate ratio ranges from 0.5 to 2.0. The experimental validations of our linear model are mainly discussed both for high ($0.1 \le C_a \le 1.0$) and low ($C_a \le 0.1$) Capillary numbers.

2. Experimental setup

A T-junction microdroplet generator is designed for droplet formation, and by regulating the flow rates of the two immiscible fluids, the size of individual droplets can be controlled. Fig. 1 shows the schematic of the T-junction microdroplet generator. To test the effects of the geometry of the microchannels on the droplet formation, two geometries of the T-junction microchannels are designed for our experiment. Table 1 shows the geometrical parameters of the T-junction microchannels 1 and 2. Here, ω_c is the channel width of the continuous phase, ω_d is the channel width of the

dispersed phase, h is the channel height of the two phases, L_d is the length of the droplets, Q_c is the flow rate of the continuous phase and Q_d is the flow rate of the dispersed phase.

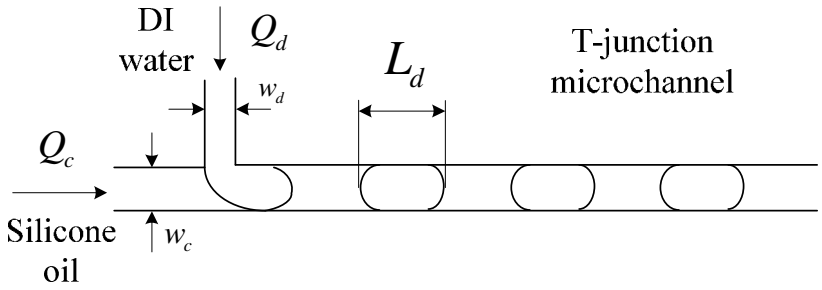

Fig. 1 Schematic of the T-junction microdroplet generator.

Table 1 Geometrical parameters of the T-junction microchannels.

Parameters	ω_c (μm)	ω_d (μm)	h (μm)
Microchannel 1	100	50	50
Microchannel 2	100	100	50

For our experiments, the flow rates of the fluids are supplied by the syringe pump (Harvard Apparatus PHD 22/2000 Syringe Pump). For the two immiscible fluids, the silicone oil is chosen as the continuous phase and the DI water is chosen as the dispersed phase. The viscosity of the DI water is μ_d = 1 cP, and three types of silicone oil (viscosity: μ_c = 20, 100, 500 cP) are tested for droplet formation, respectively. The interfacial tension γ between the two phases is approximated as: $\gamma = 40$ mN/m. During droplet formation, based on the viscosity μ_c of the continuous phase and its velocity v_c, the Capillary number is defined as $C_a = \frac{\mu_c v_c}{\gamma}$, and the experiments of droplet formation are conducted under both low and high Capillary numbers. To obtain a low Capillary number, the flow rate of the silicone oil is fixed as $Q_c = 0.01$ ml/min, while the flow rate of the DI water Q_d varies from 0.005 to 0.02 ml/min, with the flow rate ratio $0.5 \le Q_d / Q_c \le 2.0$. The Capillary number can be estimated for different viscosity of the silicone oil, as shown in Table 2. We note that under this flow conditions, droplet formation is performed at a low Capillary number ($C_a \le 0.1$). Additionally, we choose a higher flow rate of the

silicone oil $Q_c = 0.1$ ml/min, while the flow rate Q_d of the DI water ranges from 0.05 to 0.2 ml/min, with the flow rate ratio $0.5 \le Q_d / Q_c \le 2.0$. The Capillary number can be estimated for different viscosity of the silicone oil, as shown in Table 2. We note that under this flow conditions, droplet formation can be performed at a high Capillary number ($0.1 \le C_a \le 1.0$).

Table 2 Capillary number of droplet formation for different viscosity of the silicone oil. The flow rate of the silicone oil is constant: $Q_c = 0.01$ ml/min.

μ_c (cP)	μ_d (cP)	C_a
20	1	0.002
100	1	0.01
500	1	0.05

Table 3 Capillary number of droplet formation for different viscosity of the silicone oil. The flow rate of the silicone oil is constant: $Q_c = 0.1$ ml/min.

μ_c (cP)	μ_d (cP)	C_a
20	1	0.02
100	1	0.1
500	1	0.5

3. Mathematical model

In this paper, monodisperse droplets are formed in a T-junction microchannel, and the volume of the droplet can be controlled by changing the flow rates of the two immiscible fluids. Fig. 2(a) shows three dimensions of droplet generation, Fig. 2(b) shows the main parameters for two dimensions of droplet generation and Fig. 2(c) shows the cross section of the microchannel, where Q_o is the leakage flow rate of the continuous phase before the dispersed phase fully blocks the cross section of the T-junction.

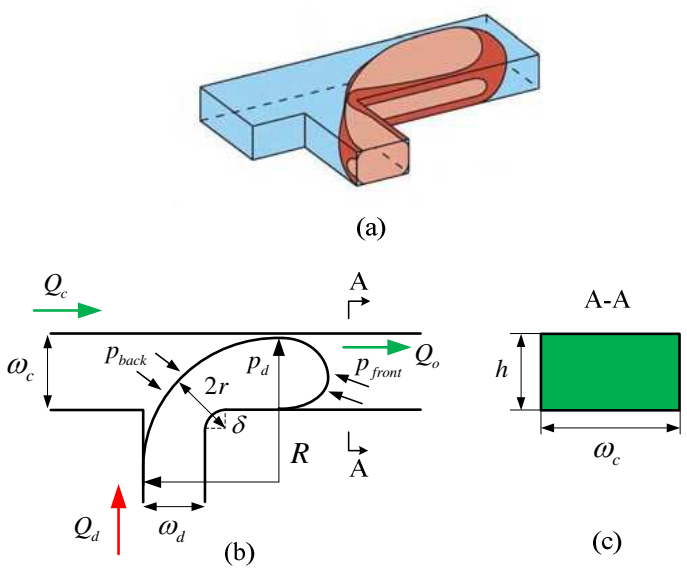

Fig. 2 (a) Three dimensions of droplet generation, (b) Two dimensions of droplet generation, (c) Cross section of the microchannel.

In a T-junction microchannel, at a low Capillary number ($C_a \leq 0.1$), the process of droplet formation can be divided into two stages: the filling stage and the squeezing stage [13,14]. For each stage, there is some contribution to the volume of the droplet, respectively, and the whole volume of each droplet can be described by

$$V_{drop} = V_{fill} + V_{squeeze} \tag{1}$$

where V_{fill} is the droplet volume of the filling stage and $V_{squeeze}$ is the droplet volume of the squeezing stage.

In this paper, to quantitatively study the relation between the droplet size and the flow-rate ratio, the droplet volume can be normalized by $w_c^2 h$ [28]. Assuming the volume of the squeezing stage as a linear function of the flow-rate ratio [14] $\frac{V_{squeeze}}{w_c^2 h} = \beta \frac{Q_d}{Q_c}$, and substituting into equation (1), the dimensionless droplet volume is given by

$$\frac{V_{drop}}{w_c^2 h} = \frac{V_{fill}}{w_c^2 h} + \beta \frac{Q_d}{Q_c} \tag{2}$$

Next, the volume of the two stages will be calculated separately. At the T-junction where the continuous phase and the dispersed phase meet, the cross section of the interface of the two phases is shown in Fig. 3.

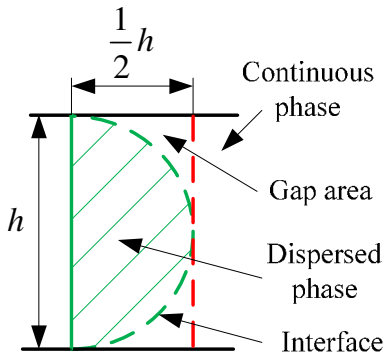

Fig. 3 Cross section of the interface of the two phases.

Then, the gap area between the two phases can be calculated

$$A_{gap} = 2\left(1-\frac{\pi}{4}\right)\left(\frac{h}{2}\right)^2 \tag{3}$$

At the T-junction, we define V_c as the volume of the continuous phase and V_d as the volume of the dispersed phase, then we have

$$\begin{cases} V_c = hA_c + cA_{gap} \\ V_d = hA_d - cA_{gap} \end{cases} \tag{4}$$

where A_c is the surface area of the continuous phase, A_d is the surface area of the dispersed phase and c is the contact length along the interface of the two phases.

During the filling stage, the dispersed phase flows into the T-junction and narrows the cross section of the continuous phase. When the flow of the continuous phase is fully blocked by the dispersed phase, it reaches the end of the filling stage, as shown in Fig. 4(a).

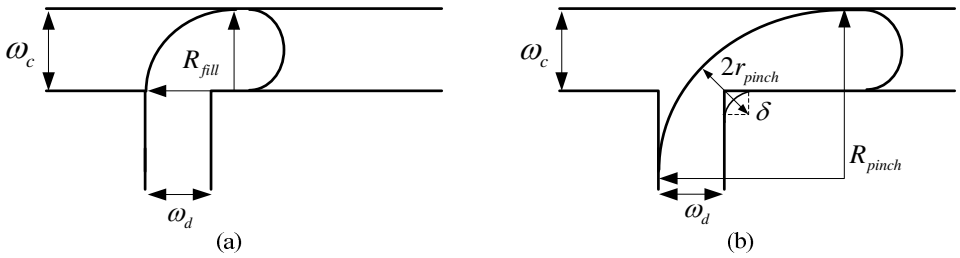

Fig. 4 (a) Final state of the filling stage, (b) Final state of the squeezing stage. R_{fill} is the radius at the beginning of the squeezing stage, R_{pinch} is the radius at the end of the squeezing stage and δ is the radius at the corner of the T-junction.

From Fig. 4(a), with $R_{fill} = w_c$, we have the surface area of the dispersed phase

$A_{fill} = \frac{3\pi}{8} w_c^2$, and the contact length $c_{fill} = \pi w_c$. Substituting into equation (4), the droplet volume of the filling stage can be described by

$$V_{fill} = \left[\frac{3\pi}{8} - \frac{\pi}{2}\left(1 - \frac{\pi}{4}\right)\frac{h}{w_c} \right] w_c^2 h \tag{5}$$

During the squeezing stage, the dispersed phase is squeezed by the continuous phase at the T-junction, and by the end of this stage, monodisperse droplets are formed because of the pinch off of the dispersed phase. Fig. 4(b) shows the final state of the squeezing stage. Assuming it takes the time Δt_s for the squeezing stage, with $\frac{V_{squeeze}}{w_c^2 h} = \beta \frac{Q_d}{Q_c}$, and the droplet volume of the squeezing stage is given by

$$V_{squeeze} = Q_d \Delta t_s = \beta w_c^2 h \frac{Q_d}{Q_c} \tag{6}$$

For the squeezing stage, as the continuous phase flows into the T-junction, the volume of the continuous phase is increasing. In particular, there is some leakage of the continuous phase during the squeezing process (see Fig. 2(b)), with the time-rate change of the volume of the continuous phase being expressed as

$$\frac{dV_c}{dt} = Q_c \left(1 - \frac{Q_o}{Q_c}\right) \tag{7}$$

where Q_o is the leakage flow rate. For our experiments of droplet formation, we can assume $Q_o / Q_c = 0.1$. For the continuous phase, by differentiating on both sides of equation (3), with the time-rate change of the volume as a function of the time-rate change of the surface area and the contact length, yields

$$\frac{dV_c}{dt} = h \frac{dA_c}{dt} + 2\left(\frac{h}{2}\right)^2 \left(1 - \frac{\pi}{4}\right)\frac{dc}{dt} \tag{8}$$

To acquire the time Δt_s for the squeezing stage, the time-rate change of the volume $\frac{dV_c}{dt}$ is associated with the time-rate change of the radius $\frac{dR}{dt}$. For the continuous phase, we have $dA_c = \left(1 - \frac{\pi}{4}\right) dR^2$, $dc = \frac{\pi}{2} dR$, and substituting into equation (7) and (8), gives the relationship

$$\frac{Q_c}{w_c^2 h}\left(1-\frac{Q_o}{Q_c}\right)=\frac{1}{w_c^2}\left(1-\frac{\pi}{4}\right)\left(2R+\frac{\pi}{4}h\right)\frac{dR}{dt} \tag{9}$$

Integrating on both sides of equation (9), with the initial radius $R = R_{fill}$ and the radius at the end of the squeezing stage $R = R_{pinch}$, yields

$$\Delta t_s = \frac{w_c^2 h}{Q_c}\left(1-\frac{\pi}{4}\right)\left(1-\frac{Q_o}{Q_c}\right)^{-1}\left[\left(\frac{R_{pinch}}{w_c}\right)^2-\left(\frac{R_{fill}}{w_c}\right)^2+\frac{\pi}{4}\frac{h}{w_c}\left(\frac{R_{pinch}}{w_c}-\frac{R_{fill}}{w_c}\right)\right] \tag{10}$$

Substituting into equation (6), the coefficient β can be obtained

$$\beta = \left(1-\frac{\pi}{4}\right)\left(1-\frac{Q_o}{Q_c}\right)^{-1}\left[\left(\frac{R_{pinch}}{w_c}\right)^2-\left(\frac{R_{fill}}{w_c}\right)^2+\frac{\pi}{4}\frac{h}{w_c}\left(\frac{R_{pinch}}{w_c}-\frac{R_{fill}}{w_c}\right)\right] \tag{11}$$

where $R_{fill} = w_c$, and R_{pinch} is still unknown. Next, we need to calculate the value of R_{pinch}. Here, we define p_{back} and p_{front} as the pressure at the back and front of the droplet, respectively (see Fig. 2(b)). Therefore, prior to pinch-off of each droplet, the static Laplace pressure jump over the interface can be described by

$$\begin{cases} p_d - p_{back} = \sigma\left(\dfrac{1}{r_{pinch}}+\dfrac{1}{R_{pinch}}\right) \\ p_d - p_{front} = 2\sigma\left(\dfrac{1}{w_c}+\dfrac{1}{h}\right) \end{cases} \tag{12}$$

where p_d represents the pressure inside the droplet. Assuming the pressure inside the droplet is constant, therefore, at the pinch-off point of each droplet, we have $p_{back} = p_{front}$, and substituting into equation (12), with $R_{pinch} >> r_{pinch}$ yields the approximation

$$r_{pinch} = \frac{1}{2}\frac{hw_c}{h+w_c} \tag{13}$$

From Fig. 4(b), the geometrical relation between R and r is given by

$$2r_{pinch} - \delta = R_{pinch} - \sqrt{\left(R_{pinch}-w_c\right)^2+\left(R_{pinch}-w_d\right)^2} \tag{14}$$

Substituting equation (13) into (14), the R_{pinch} of the droplet pinch-off is obtained

$$R_{pinch} = w_c + w_d + \delta - \frac{hw_c}{h+w_c} + \left[2\left(w_c + \delta - \frac{hw_c}{h+w_c} \right)\left(w_d + \delta - \frac{hw_c}{h+w_c} \right) \right]^{\frac{1}{2}} \quad (15)$$

For our design of the T-junction microchannel, it can be approximated $\delta \approx 2\,\mu$m. From the two dimensional model of the droplet (see Fig. 1), the relation between the droplet volume V_{drop} and the droplet length L_d is approximately described by

$$V_{drop} = \left[L_d w_c - \left(1 - \frac{\pi}{4} \right) w_c^2 \right] h \quad (16)$$

Substituting equation (16) and (5) into equation (2), the relation between the droplet length L_d / w_c and the flow-rate ratio Q_d / Q_c is given by [12]

$$\frac{L_d}{w_c} = \alpha + \beta \frac{Q_d}{Q_c} \quad (17)$$

where $\alpha = 1 + \frac{\pi}{8} - \frac{\pi}{2}\left(1 - \frac{\pi}{4} \right)\frac{h}{w_c}$ and β is obtained from equation (11).

We note that the droplet length L_d / w_c is a linear function of the flow-rate ratio Q_d / Q_c, especially, the coefficients of the linear equation are determined by the geometrical parameters of the microchannel, and independent of the viscosity of the fluids.

4. Results and discussion

4.1 Measurements of droplet size at a low Capillary number ($C_a \le 0.1$)

To testing the linear relation between the droplet length and the flow-rate ratio, the experiments of droplet formation are conducted at a low Capillary number ($C_a \le 0.1$). As the flow rate of the silicone oil is constant: $Q_c = 0.01$ ml/min, and by increasing the flow-rate ratio from 0.5 to 2.0, the length of the droplets is measured experimentally. For the T-junction microchannel 1 ($w_d / w_c = 0.5$), as the viscosity of the silicone oil varies from 20 to 500 cP, the droplet length as a function of the flow-rate ratio is obtained, as shown in Fig. 5. For the T-junction microchannel 2 ($w_d / w_c = 1.0$), as the viscosity of the silicone oil varies from 20 to 500 cP, the droplet length as a function of the flow-rate ratio is obtained, as shown in Fig. 6.

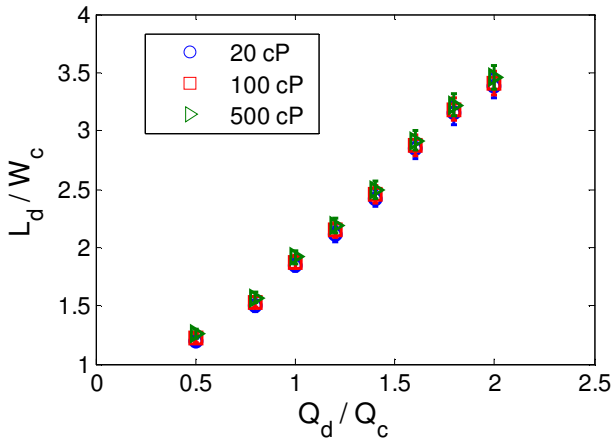

Fig. 5 Relation between the droplet length L_d/w_c and the flow rate ratio Q_d/Q_c for different viscosity of the silicone oil. All the experiments of droplet formation are performed in the T-junction microchannel 1 for $C_a \le 0.1$.

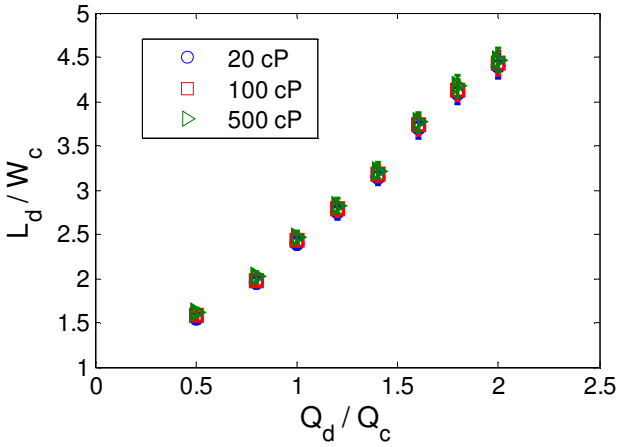

Fig. 6 Relation between the droplet length L_d/w_c and the flow rate ratio Q_d/Q_c for different viscosity of the silicone oil. All the experiments of droplet formation are performed in the T-junction microchannel 2 for $C_a \le 0.1$.

We observe that for different viscosity of the silicone oil, the droplet length L_d/w_c is approximately a linear function of the flow-rate ratio Q_d/Q_c. In particular, for a typical flow-rate ratio, the droplet length barely varies with the viscosity of the silicone oil. As a result, at a low Capillary number ($C_a \le 0.1$), the effects of the viscosity of the fluids on the droplet size are negligible.

In addition, both for the T-junction microchannel 1 ($w_d/w_c = 0.5$) and 2 ($w_d/w_c = 1.0$), with viscosity of the DI water μ_d = 1 cP and viscosity of the silicone

oil μ_c = 500 cP for $C_a = 0.05$, the droplet length are measured for different flow-rate ratios, which are compared with the theoretical predictions, as shown in Fig. 7.

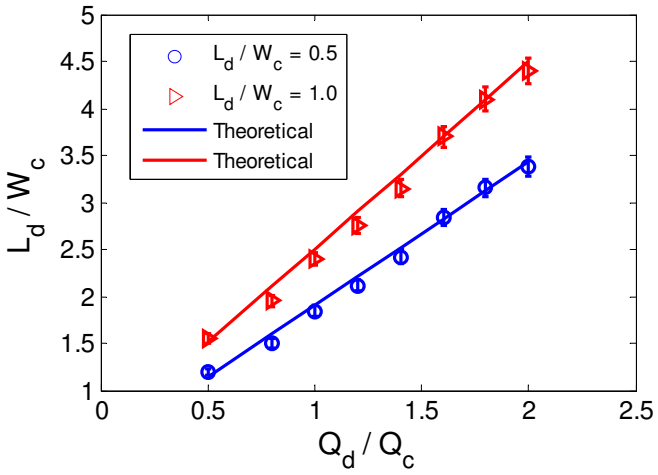

Fig. 7 Linear relation between the droplet length L_d/w_c and the flow rate ratio Q_d/Q_c for two geometries of the T-junction microchannels. The viscosity of the DI water is μ_d = 1 cP, the viscosity of the silicone oil is μ_c = 500 cP and the Capillary number is $C_a = 0.05$. The solid lines represent the theoretical predictions of L_d/w_c.

We note that the linear relation between the droplet length L_d/w_c and flow-rate ratio Q_d/Q_c is depend on the geometrical parameters of the T-junction microchannel. More importantly, it can be observed that for a specific flow-rate ratio, the experimental measurements of the droplet length coincide with the theoretical predictions of the droplet length both for the T-junction microchannel 1 ($w_d/w_c = 0.5$) and 2 ($w_d/w_c = 1.0$). As a result, the linear model of droplet formation can be verified experimentally for low Capillary numbers. Especially, the coefficients of the linear model can be predicted by the geometrical parameters of a T-junction microchannel.

4.2 Measurements of droplet size at a high Capillary number ($0.1 \le C_a \le 1.0$)

In addition to validate the linear model of droplet formation at a low Capillary number ($C_a \le 0.1$), the relation between the droplet length and the flow-rate ratio is also measured experimentally at a high Capillary number ($0.1 \le C_a \le 1.0$). As the

flow rate of the silicone oil is fixed as: $Q_c = 0.1$ ml/min, with the flow-rate ratio Q_d/Q_c increasing from 0.5 to 2.0, the length of the droplets is measured experimentally. For the T-junction microchannel 1 ($w_d/w_c = 0.5$), with viscosity of the silicone oil μ_c = 500 cP and for $C_a = 0.5$, the droplet length are measured for different flow-rate ratios, which are compared with the theoretical predictions, as shown in Fig. 8. For the T-junction microchannel 2 ($w_d/w_c = 1.0$), with viscosity of the silicone oil μ_c = 500 cP and for $C_a = 0.5$, the droplet length are measured for different flow-rate ratios, which are compared with the theoretical predictions, as shown in Fig. 9.

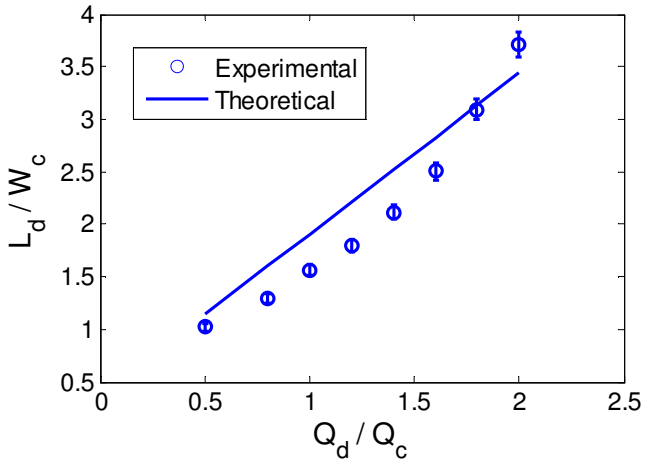

Fig. 8 Relation between the droplet length L_d/w_c and the flow rate ratio Q_d/Q_c for the T-junction microchannel 1. The viscosity of the DI water is μ_d = 1 cP, the viscosity of the silicone oil is μ_c = 500 cP and the Capillary number is $C_a = 0.5$. The solid line represents the theoretical predictions of L_d/w_c.

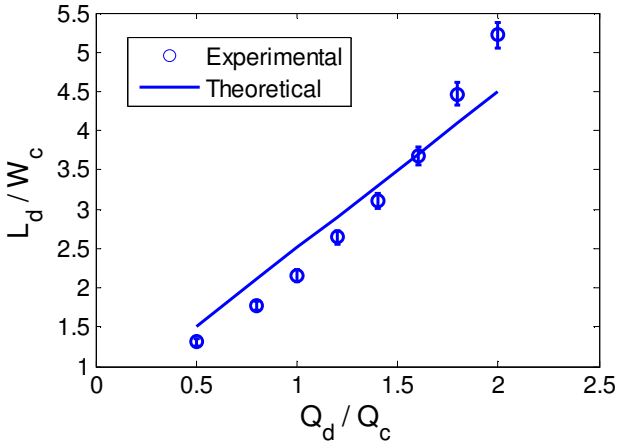

Fig. 9 Relation between the droplet length L_d/w_c and the flow rate ratio Q_d/Q_c for the T-junction microchannel 2. The viscosity of the DI water is μ_d = 1 cP, the viscosity of the silicone oil is μ_c = 500 cP and the Capillary number is C_a = 0.5 . The solid line represents the theoretical predictions of L_d/w_c .

From the experimental results, we observe the measured droplet length L_d/w_c varies nonlinearly with the flow-rate ratio Q_d/Q_c at a high Capillary number ($0.1 \le C_a \le 1.0$). By comparing the experimental measurements of the droplet length with the theoretical predictions, we note there is some deviation between the predicted and measured values of L_d/w_c under the same flow-rate ratio Q_d/Q_c. In particular, the nonlinearity between L_d/w_c and Q_d/Q_c is becoming more significant at higher flow-rate ratios. Therefore, for the T-junctions, the droplet length cannot be assumed as a linear function of the flow-rate ratio for high Capillary numbers.

5. Conclusions

For a T-junction microdroplet generator, a mathematical model which describes the linear relation between the droplet length L_d/w_c and the flow-rate ratio Q_d/Q_c is established. From both theoretical and experimental study, the droplet length varies linearly with the flow-rate ratio for different Capillary numbers ($C_a \le 0.1$), and especially, the linear relation which is independent of the viscosity of the fluids, can be determined by the geometrical parameters of a T-junction microchannel. However,

from experimental measurements, the droplet length is a nonlinear function of the flow-rate ratio for high Capillary numbers ($0.1 \le C_a \le 1.0$). As a result, for $C_a \le 0.1$, the linear model of droplet formation can be validated experimentally. In particular, the coefficients α and β of the linear equation can be calculated for different geometries of the T-junctions, and the size of individual droplets can be accurately predicted for a certain flow-rate ratio. Most importantly, by improving the control accuracy of the flow rates of the two phases, high uniformity and precision of droplet formation can be achieved for the T-junction microdroplet generators.

Acknowledgements
This work was supported by the National Natural Science Foundation of China (No: 51175101) and the Programme of Introducing Talents of Discipline to Universities (No: B07018). The authors thank Professor Howard A. Stone and Doctor Ian Jacobi at Princeton University for their technical support and suggestions.

References

[1] J. El-Ali, P. K. Sorger and K. F. Jensen. Cells on chips. Nature, 2006, 442, 403-411.
[2] Liat Rosenfeld, Lin Fan, Yunhan Chen, Ryan Swoboda and Sindy K. Y. Tang. Break-up of droplets in a concentrated emulsion flowing through a narrow constriction. Soft Matter, 2014, 10, 421-430.
[3] Jinmu Jung and Jonghyun Oh. Cell-induced flow-focusing instability in gelatin methacrylate microdroplet generation. Biomicrofludics, 2014, 8, 036503.
[4] D. B. Weibel and G. M. Whitesides. Applications of microfluidics in chemical biology. Curr. Opin. Chem. Biol., 2006, 12, 584-591.
[5] J. deMell. Control and detection of chemical reactions in microfluidic systems. Nature, 2006, 442, 394-402.
[6] Michael M. Fryd and Thomas G. Mason. Self-limiting droplet fusion in ionic emulsions. Soft Matter, 2014, 10, 4662-4673.
[7] Zhan Y H, Wang J, Bao N and Lu C. Electroporation of cells in microfluidic droplets. Anal. Chem., 2009, 81, 2027-2031.
[8] Elisabeth Rondeau and Justin J. Cooper-White. Formation of multilayered biopolymer microcapsules and microparticles in a multiphase microfluidic flow. Biomicrofludics, 2012, 6, 024125.
[9] Tushar D. Rane, Helena C. Zec, Chris Puleo, Abraham P. Lee and Tza-Huei Wang. Droplet microfluidics for amplification-free genetic detection of single cells. Lab on a Chip, 2012, 12, 3341-3347.
[10] Mira T. Guo, Assaf Rotem, John A. Heyman and David A. Weitz. Droplet microfluidics for high-throughput biological assays. Lab on a Chip, 2012, 12, 2146-2155.
[11] Thomas Ward, Magalie Faivre, Manouk Abkarian and Howard A. Stone. Microfluidic flow focusing: Drop size and scaling in pressure versus flow-rate-driven pumping. Electrophoresis, 2005, 26, 3716-3724.

[12] Piotr Garstecki, Michael J. Fuerstman, Howard A. Stone and George M. Whitesides. Formation of droplets and bubbles in a microfluidic T-junction-scaling and mechanism of break-up. Lab on a Chip, 2006, 6, 437-446.

[13] Tomasz Glawdel, Caglar Elbuken, and Carolyn L. Ren. Droplet formation in microfluidic T-junction generators operating in the transitional regime: experimental observations. Physical Review E, 2012, 85, 016322.

[14] Tomasz Glawdel, Caglar Elbuken, and Carolyn L. Ren. Droplet formation in microfluidic T-junction generators operating in the transitional regime: modeling. Physical Review E, 2012, 85, 016323.

[15] Razieh Kebriaei and Amar S. Basu. Autosizing closed-loop drop generator using morphometric image feedback. International Conference on Miniaturized Systems for Chemistry and Life Sciences, 2013, 1944-1946.

[16] Piotr M. Korczyk, Olgierd Cybulski,a Sylwia Makulskaa and Piotr Garstecki. Effects of unsteadiness of the rates of flow on the dynamics of formation of droplets in microfluidic systems. Lab Chip, 2011, 11, 173-175.

[17] Piotr Garstecki, Irina Gitlin, Willow DiLuzio, George M. Whitesides, Eugenia Kumacheva and Howard A. Stone. Formation of monodisperse bubbles in a microfluidic flow-focusing device. Applied Physics Letters, 2004, 10, 2649-2651.

[18] Erik Miller, Mario Rotea, and Jonathan P. Rothstein. Microfluidic device incorporating closed loop feedback control for uniform and tunable production of micro-droplets. Lab on a Chip, 2010, 10, 1293-1301.

[19] Todd M. Moyle, Lynn M. Walker and Shelley L. Anna. Controlling thread formation during tipstreaming through an active feedback control loop. Lab on a Chip, 2013, 13, 4534-4541.

[20] Shiying Wang, Ali H. Dhanaliwala, Johnny L. Chen, and John A. Hossack. Production rate and diameter analysis of spherical monodisperse microbubbles from two-dimensional expanding-nozzle flow-focusing microfluidic devices. Biomicrofluidics, 2013, 7, 014103.

[21] Yiping Hong and Fujun Wang. Flow rate effect on droplet control in a co-flowing microfluidic Device. Microfluid Nanofluid, 2007, 3, 341-346.

[22] Zhihong Nie, MinsSeok Seo, Shengqing Xu, Patrick C. Lewis, Michelle Mok, Eugenia Kumacheva, George M. Whitesides, Piotr Garstecki and Howard A. Stone. Emulsification in a microfluidic flow-focusing device: effect of the viscosities of the liquids. Microfluid Nanofluid, 2008, 5, 585-594.

[23] Gordon F. Christopher, N. Nadia Noharuddin, Joshua A. Taylor and Shelley L. Anna. Experimental observations of the squeezing-to-dripping transition in T-shaped microfluidic junctions. Physical Review E, 2008, 78, 71-79.

[24] J. H. Xu and S. W. Li and J. Tan and G. S. Luo. Correlations of droplet formation in T-junction microfluidic devices: from squeezing to dripping. Microfluid Nanofluid, 2008, 5, 711-717.

[25] M. Demenech, P. Garstecki, F. Jousse and H. A. Stone. Transition from squeezing to dripping in a microfluidic T-shaped junction. J. Fluid Mech., 2008, 595, 141-161.

[26] Amar S. Basu. Droplet morphometry and velocimetry (DMV): a video processing software for time-resolved, label-free tracking of droplet parameters. Lab on a Chip, 2013, 13, 1892-1901.

[27] Caglar Elbuken, Tomasz Glawdel, Danny Chan, Carolyn L. Ren. Detection of microdroplet size and speed using capacitive sensors. Sens. Actuator A: Phys., 2011, 171, 55-62.

[28] Tomasz Glawdel and Carolyn L. Ren. Global network design for robust operation of

microfluidic droplet generators with pressure-driven flow. Microfluid Nanofluid, 2012, 13, 469-480.